




## ORIGINAL ARTICLE

# A *Phytophthora capsici* RXLR effector manipulates plant immunity by targeting RAB proteins and disturbing the protein trafficking pathway

Tianli Li<sup>1</sup>  | Gan Ai<sup>1</sup>  | Xiaowei Fu<sup>1</sup> | Jin Liu<sup>1</sup> | Hai Zhu<sup>1</sup> | Ying Zhai<sup>2</sup> |  
Weiye Pan<sup>1</sup> | Danyu Shen<sup>1</sup> | Maofeng Jing<sup>1</sup> | Ai Xia<sup>1</sup> | Daolong Dou<sup>1</sup> 

<sup>1</sup>College of Plant Protection, Academy for Advanced Interdisciplinary Studies, Nanjing Agricultural University, Nanjing, China

<sup>2</sup>Department of Plant Pathology, Washington State University, Pullman, Washington, USA

## Correspondence

Daolong Dou, College of Plant Protection, Academy for Advanced Interdisciplinary Studies, Nanjing Agricultural University, Nanjing, China.

Email: [ddou@njau.edu.cn](mailto:ddou@njau.edu.cn)

## Funding information

Fundamental Research Funds for the Central Universities, Grant/Award Number: JCQY201904 and KYT202001; National Natural Science Foundation of China, Grant/Award Number: 31625023, 32072507, 32070139 and 31721004

## Abstract

The oomycete pathogen *Phytophthora capsici* encodes hundreds of RXLR effectors that enter the plant cells and suppress host immunity. Only a few of these genes are conserved across different strains and species. Such core effectors might target hub genes and immune pathways in hosts. Here, we describe the functional characterization of the core *P. capsici* RXLR effector RXLR242. The expression of RXLR242 was up-regulated during infection, and its ectopic expression in *Nicotiana benthamiana*, an experimental plant host, further promoted *Phytophthora* infection. RXLR242 physically interacted with a group of RAB proteins that belong to the small GTPase family and play a role in regulating transport pathways in the intracellular membrane trafficking system. In addition, RXLR242 impeded the secretion of PATHOGENESIS-RELATED 1 (PR1) protein to the apoplast. This phenomenon resulted from the competitive binding of RXLR242 to RABE1-7. We also found that RXLR242 interfered with the association between RABA4-3 and its binding protein, thereby disrupting the trafficking of the membrane receptor FLAGELLIN-SENSING 2. Thus, RXLR242 manipulates plant immunity by targeting RAB proteins and disrupting protein trafficking in the host plants.

## KEYWORDS

FLS2, *Phytophthora*, plant immunity, PR1, protein trafficking, RAB GTPase, RXLR effector

## 1 | INTRODUCTION

Unlike mammals, plants lack internal specialized immune cells to defend against pathogens. Instead, they rely on the innate immunity of the individual cells and have evolved a sophisticated signal transduction network to respond to pathogens (Jones & Dangl, 2006). For example, protein receptors localized on the plant cell

membrane can detect conserved pathogen-associated molecular patterns (PAMPs), leading to an immune response cascade, such as the rapid release of reactive oxygen species (Tsuda & Katagiri, 2010). Plants also secrete defence molecules into apoplasts to combat pathogen invasion (Doehlemann & Hemetsberger, 2013). Pathogens can secrete effectors to overcome the host immunity and establish an infection (Dou & Zhou, 2012; Latijnhouwers

Tianli Li and Gan Ai contributed equally to this article.

This is an open access article under the terms of the [Creative Commons Attribution-NonCommercial-NoDerivs](https://creativecommons.org/licenses/by-nc-nd/4.0/) License, which permits use and distribution in any medium, provided the original work is properly cited, the use is non-commercial and no modifications or adaptations are made.

© 2022 The Authors. *Molecular Plant Pathology* published by British Society for Plant Pathology and John Wiley & Sons Ltd.

et al., 2003). These secreted effectors target hub genes and critical processes in the plant immune network (Mukhtar et al., 2011; Petre et al., 2021; Win et al., 2019). Thus, unravelling the mechanisms underlying these effector-target associations might help to identify the critical host-pathogen interactions and design efficient disease control strategies.

Oomycetes comprise a class of filamentous pathogens that infect both plants and animals (Latijnhouwers et al., 2003). Their genomes encode several effectors and are, therefore, ideal systems to investigate effector-target associations (Jiang et al., 2008; Win et al., 2007). *Phytophthora*, an oomycete genus comprising over 120 species, includes some of the most devastating plant pathogens (Kamoun et al., 2015). *Phytophthora* pathogens secrete effectors into host cells via infection structures called haustoria, which establish intimate contact with the host plants. The largest cytoplasmic effectors in *Phytophthora* contain a conserved N-terminal Arg-X-Leu-Arg (RXLR) motif (Jiang et al., 2008; Win et al., 2007). Each *Phytophthora* species encodes 300–700 RXLR effectors (Jiang et al., 2008; Win et al., 2007), many of which can compromise plant host disease resistance when expressed ectopically. Some RXLR effectors suppress plant defences by targeting specific proteins that mediate host immunity (Boevink et al., 2016; Wang & Wang, 2018). However, the host targets and virulence mechanisms of most RXLR effectors remain unclear.

RXLRs exhibit considerable intra- and interspecies diversity. Only 16 homologous RXLRs are shared between *Phytophthora sojae*, *P. ramorum*, and *P. infestans* (Haas et al., 2009). Such conserved effectors are also called core effectors and might be vital for successful *Phytophthora* infection. Exploring the virulence mechanism of core effectors will shed light on the critical interactions between *Phytophthora* pathogens and their hosts.

The protein trafficking pathway is disturbed by multiple effectors because of its critical role in plant immunity (Du et al., 2015; Schmidt et al., 2014; Tomczynska et al., 2018). Filamentous pathogens, such as fungi and oomycetes, extend their hyphae into the intercellular space between plant cells. The plants, in turn, respond by secreting antagonists, including antimicrobial proteins, enzyme inhibitors, hydrolytic enzymes, and metabolites (Kwon et al., 2008). Vesicle trafficking serves as a transportation network that relocates these compounds to their destinations. It is responsible for immune receptor transportation, defence signalling, and targeting antagonist cargo to the pathogen invasion sites (Beck et al., 2012; Frei dit Frey & Robatzek, 2009; Gu et al., 2017).

Ras-associated binding (RAB) guanosine triphosphate hydrolases (GTPases) play an important role in specifying transport pathways in eukaryotic intracellular membrane trafficking systems (Minamino & Ueda, 2019). In vesicle trafficking, RAB GTPases regulate the budding and docking steps of vesicles to their target membranes. They may also transport defence proteins from the endoplasmic reticulum (ER) to the plasma membrane (PM) or apoplasts, thereby regulating plant innate immunity. For example, the RAB GTPase RAB1d stimulates the secretion of

PATHOGENESIS-RELATED 1 (PR1) protein (Speth et al., 2009). By contrast, RABA4c and RABA6a function in distinct endocytic trafficking steps of the membrane receptor FLAGELLIN-SENSING 2 (FLS2) (Choi et al., 2013). A conserved RXLR effector targets members of the RABA GTPase and prevents the secretion of defence-related proteins (Tomczynska et al., 2018). These findings provide a glimpse into the functions of RAB proteins in host defence. However, the mechanism through which RXLR effectors disturb the RAB-mediated vesicle trafficking pathway remains obscure.

Here, we characterized a core RXLR effector, RXLR242, from *Phytophthora capsici*, an important plant-pathogenic oomycete that infects various Solanaceae and Cucurbitaceae crops (Hausbeck & Lamour, 2004). The expression of RXLR242 was up-regulated during infection. Its ectopic expression in *Nicotiana benthamiana* promoted *P. capsici* infection, and RXLR242 interacted with multiple RAB GTPases, among which RAB1-7 mediates PR1 secretion to the apoplasts. The formation of vesicle-related protein complexes and PR1 secretion was inhibited by the competitive interaction between RXLR242 and RAB1-7. Furthermore, RXLR242 also competitively targeted RABA4-3 to interfere with FLS2 trafficking. Our findings showed that RXLR242 manipulates plant immunity by targeting RAB proteins and disturbing the protein transport pathways in plant hosts.

## 2 | RESULTS

### 2.1 | RXLR242 promotes *Phytophthora* infection in *N. benthamiana*

*Phytophthora* pathogens contain large RXLR effector repertoires, each species encoding hundreds of RXLR effectors (Haas et al., 2009; Jiang et al., 2008). However, only a few RXLR effectors are conserved across *Phytophthora* species. Comparative sequence analysis has shown that 16 homologous RXLRs are shared by *P. sojae*, *P. ramorum*, and *P. infestans* (Haas et al., 2009). Moreover, RXLRs exhibit intraspecies diversity. For instance, nearly 30% of the RXLR effectors have been identified in all 29 sequenced *P. sojae* genomes (Zhang et al., 2019). We identified RXLR242 from *P. capsici*, which is a highly conserved inter- and intraspecies effector. RXLR242 is a typical RXLR effector cloned from *P. capsici* strain LT263. This effector contains a secretory signal peptide (SP) and a typical N-terminal RXLR-dEER motif (Figure S1a). Multiple sequence alignment and phylogenetic analysis revealed that RXLR242 is conserved among sequenced *P. capsici* strains (Figure S1b,c), suggesting that it is an essential effector. A sequence similarity search revealed widely distributed RXLR242 orthologues among *Phytophthora* species (cut-off <1e-10), but not in fungi or other organisms (Figure S2a,b). All RXLR242 orthologues contained an SP and RXLR-dEER motif (Figure S2a). The expression of RXLR242 was significantly up-regulated in *N. benthamiana* at the early stages (3–18h postinoculation [hpi]) of *P. capsici* infection, followed by a gradual decline

(24–48 hpi) (Figure 1a). These results suggest that RXLR242 is associated with *P. capsici* virulence.

To further analyse the role of RXLR242 in *Phytophthora* virulence, *N. benthamiana* leaves overexpressing GFP-RXLR242 (without SP; Figure S1a) and the GFP-only control were challenged with *P. capsici* strain LT263 or *Phytophthora infestans* strain TDT-88069. The western blot analysis confirmed the expression of GFP and GFP-RXLR242 (Figure 1b). In addition, GFP-RXLR242 significantly promoted the infection of *N. benthamiana* with both oomycetes, which resulted in larger leaf lesions compared with the GFP control (Figure 1c,d). These findings indicate that RXLR242 enhances *Phytophthora* infection in plants.

## 2.2 | RXLR242-associated virulence is governed by its subcellular localization in the ER membrane and nucleus

The fluorescence emission of GFP-RXLR242 transiently expressed in *N. benthamiana* leaves was consistent with that of an ER membrane marker, RFP-HDEL (Figure 2a). We also detected GFP-RXLR242 in the nucleus (Figure 2a). To further evaluate the contribution of the subcellular localization to RXLR242 activity, the N-terminus of GFP-RXLR242 was fused with a nuclear localization signal (NLS-GFP-RXLR242) (Figure S1a). The expression of the indicated proteins was confirmed by western blot analysis (Figure S3). Compared to

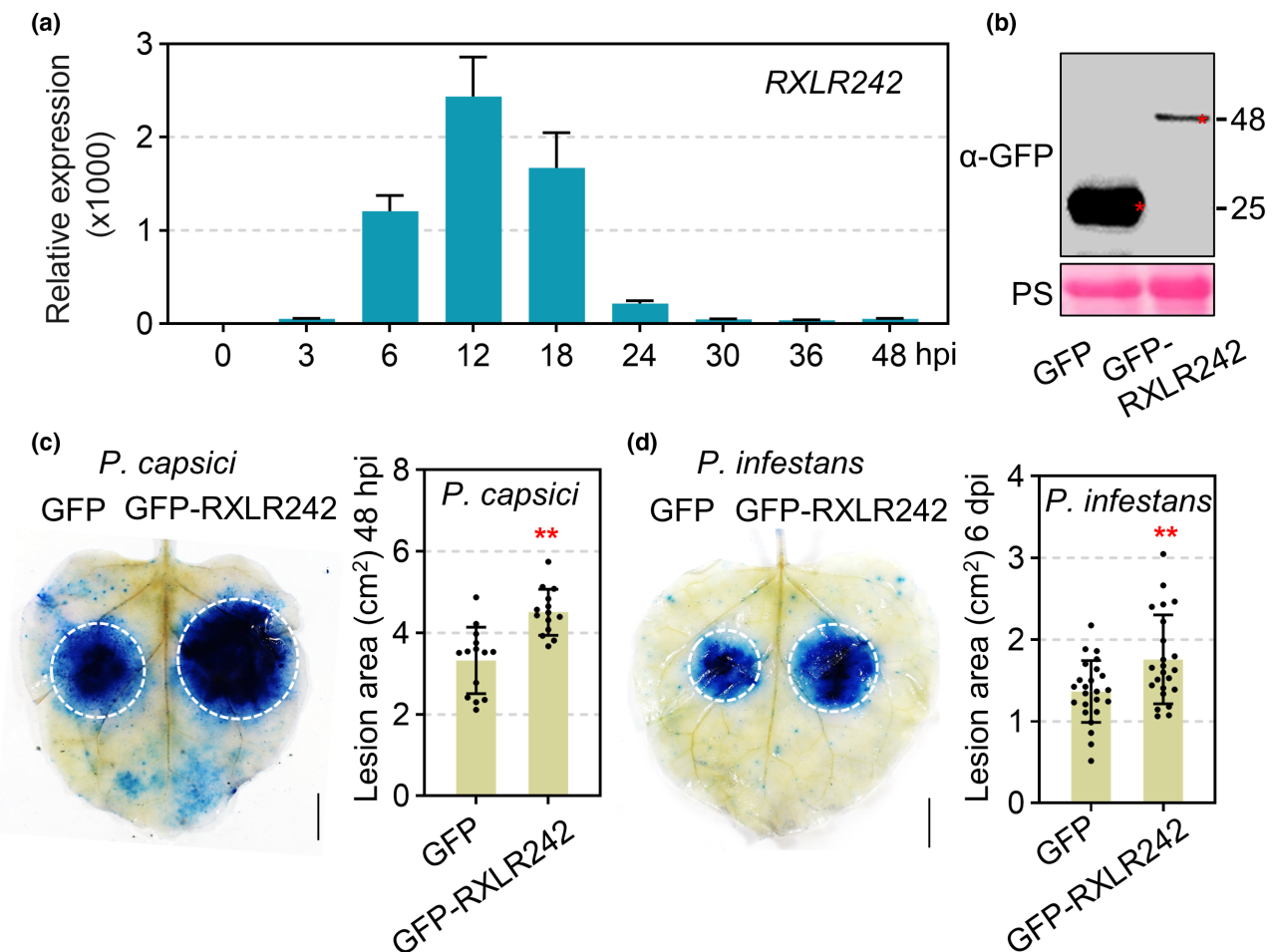


**FIGURE 1** *Phytophthora capsici* RXLR242 promotes oomycete pathogen infection. (a) Relative transcript accumulation levels of RXLR242 during infection. *Nicotiana benthamiana* leaves were challenged with *P. capsici*. RNA samples were extracted at indicated times (h postinoculation, hpi). The relative expression of RXLR242 was analysed using reverse transcription-quantitative PCR and *PcACTIN* was used as the reference (mean  $\pm$  SD,  $n = 3$ ). (b) Immunoblot analysis. The  $\alpha$ -GFP (green fluorescent protein) antibody was used to detect expression of the indicated constructs. Equal loading of each sample is indicated by Ponceau S staining (PS) of the RuBisCO protein. (c) Enhanced *P. capsici* infection in *N. benthamiana* leaves expressing RXLR242. The infiltrated area expressing GFP or GFP-RXLR242 was infected with *P. capsici*. The leaves expressing indicated constructs for 24 h were inoculated with *P. capsici*. The inoculated leaves were collected at 48 hpi for trypan blue staining and photographs were taken at bright field. Scale bar = 1 cm. Lesion areas at 48 hpi were calculated from three biological replicates using at least four leaves in each replicate (mean  $\pm$  SD,  $n > 13$ , \*\* $p < 0.01$ , Student's  $t$  test). (d) Enhanced *P. infestans* infection in *N. benthamiana* leaves expressing RXLR242. The infiltrated area expressing GFP or GFP-RXLR242 was infected with *Phytophthora infestans*. The leaves expressing indicated constructs for 24 h were inoculated with *P. infestans*. The inoculated leaves were collected at 6 days postinoculation (dpi) for trypan blue staining and photographs were taken at bright field. Scale bar = 1 cm. Lesion areas at 6 dpi were calculated from three biological replicates using at least seven leaves in each replicate (mean  $\pm$  SD,  $n > 21$ , \*\* $p < 0.01$ , Student's  $t$  test).

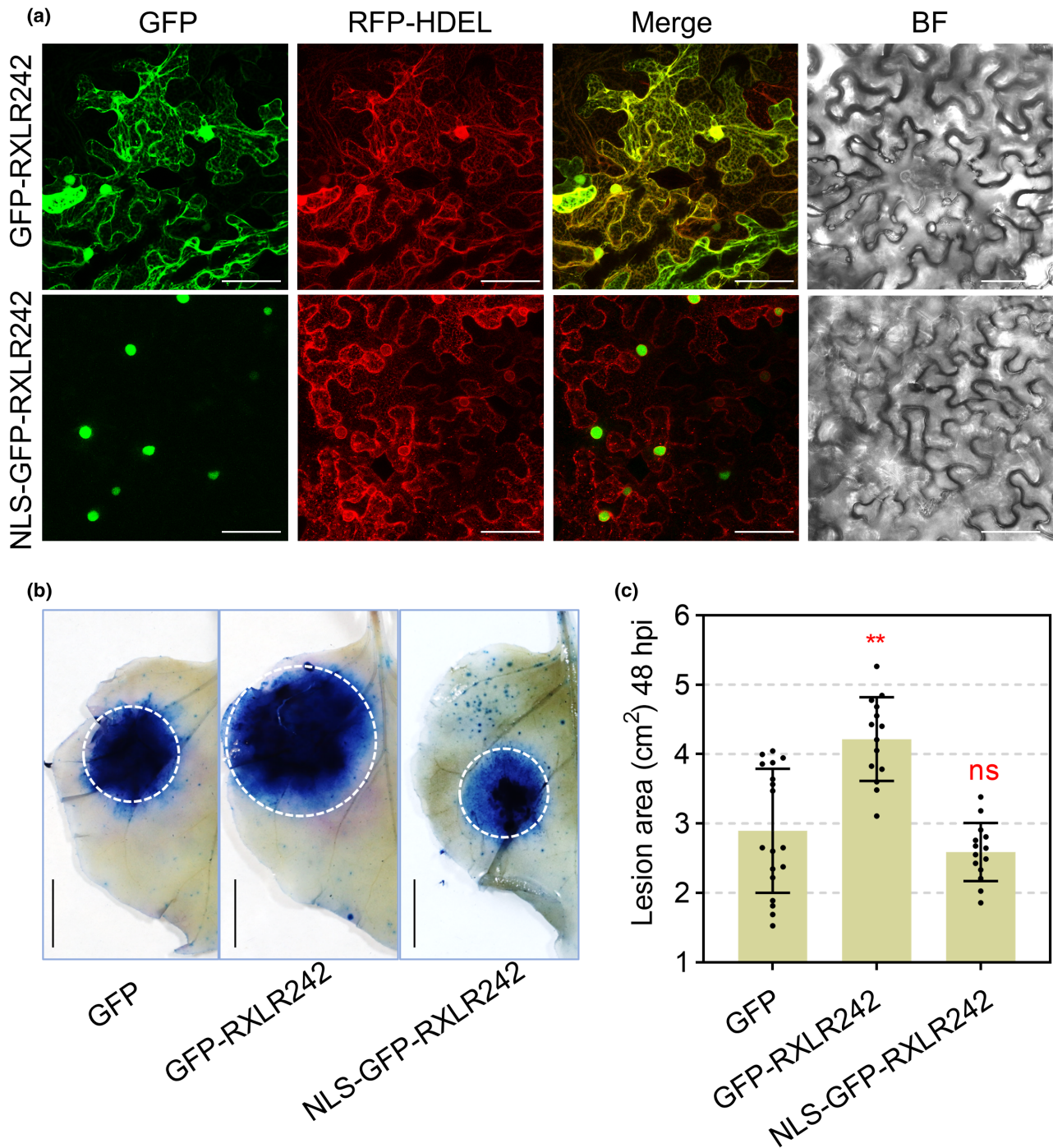


**FIGURE 2** RXLR242 virulence requires subcellular localization in the endoplasmic reticulum membrane and nucleus. (a) Subcellular localizations of GFP-RXLR242 and the mutant. Indicated constructs were expressed in *Nicotiana benthamiana* through agroinfiltration. Confocal microscopy images of leaves were taken at 48 h postinfiltration (hpi) using a 20 $\times$  lens. Each confocal microscopy picture represents a stack of five single slices. Scale bars = 50  $\mu$ m. (b, c) The infiltrated areas expressing GFP or GFP-RXLR242 or indicated mutant with nuclear localization signal (NLS) were infected with *Phytophthora capsici*. The infiltrated area expressing GFP or GFP-RXLR242 or NLS-GFP-RXLR242 for 24 h was inoculated with *P. capsici* and leaves were collected at 48 hpi for trypan blue staining. The photographs were taken at bright field (b). Lesion areas at 48 hpi (c) were calculated from three biological replicates using at least four leaves in each replicate (mean  $\pm$  SD,  $n > 12$ , \*\* $p < 0.01$ , Student's *t* test).

GFP-RXLR242, NLS-GFP-RXLR242 was found only in the nucleus, indicating its relocalization directed by the signal (Figure 2a). The quantified lesion areas showed that the GFP-RXLR242-associated

virulence was lost in NLS-GFP-RXLR242 (Figure 2b,c). These results suggest that ER membrane localization is a prerequisite for RXLR242-associated virulence.

## 2.3 | RXLR242 physically interacts with RAB GTPases

We investigated the interacting partners of GFP-RXLR242 in the host *N. benthamiana*. Transiently expressed GFP-RXLR242 in *N. benthamiana* leaves was immunoprecipitated using anti-GFP affinity beads. The negative control was transiently expressed GFP. Comparative mass spectrometry (MS) identified 144 putative *N. benthamiana* proteins that were specifically associated with GFP-RXLR242 (Figure S4 and Table S1), among which 62 proteins belonging to the RAB GTPase family were chosen for further analysis (Figure S4).

The RAB proteins in *N. benthamiana* have not been investigated at the genome-wide level, therefore we aimed to characterize and classify the protein family and phylogenetics of RXLR242-targeted RABs. We first identified all 84 NbRABs encoded in the *N. benthamiana* genome using hidden Markov models (HMMs) and standard protein BLAST (BLASTp) (Figure S5a,b and Table S2). Compared to *Arabidopsis thaliana*, RAB gene expansion has occurred in *N. benthamiana* and *Nicotiana tabacum* (Figure S5b,c). The phylogenetic analysis with AtRABs as a reference revealed that the 84 NbRABs belonged to eight subfamilies (RABA-H), with RABB and D-F being largely expanded (Figure S5d,e).

The proteins (1–28) in all subfamilies, except RABC, were identified as RXLR242 interactors by immunoprecipitation mass spectrometry (IP-MS) (Table S2), indicating a broad association of RXLR242 with RABs. These findings were supported by luciferase complementation assays (LCA), which showed interactions between RXLR242 and RABA4-3, RABD2-1, RABE1-7, RABG1-1, and RABH1-3 (Figure 3a). Notably, RABB1-2 was pulled down as an RXLR242 interactor in the IP-MS but not in the LCA (Figure 3a). Thus, RABB1-2 was considered a false-positive interactor and we therefore, included it as a negative control in the subsequent experiments.

We focused on the RABE family because the proteins in this family are involved in trafficking defence-related proteins (Speth et al., 2009). Among 11 NbRABE subfamily proteins, RABE1-1/4/5/7/11 were identified by IP-MS as RXLR242 interactors (Table S2). Among them, RABE1-7 was further analysed because *P. parasitica* inoculation induces its strongest up-regulation (Yu et al., 2019) (Table S2). Both co-immunoprecipitation (Co-IP) and pull-down assay findings confirmed the interaction between RXLR242 and RABE1-7 in vivo and in vitro, respectively (Figure 3b,c). RABE1-7 located in ER membrane (Figure S6a). The interaction between RABE1-7 and RXLR242 occurred in the ER membrane as revealed by a bimolecular fluorescence complementation (BiFC) assay (Figures 3d and S6b).

## 2.4 | Plant resistance to *P. capsici* is positively regulated by RABE1-7

To investigate the role of RABE1-7 in plant immunity, we knocked down RABE1-7 in *N. benthamiana* via RNA interference (RNAi).

Notably, RABE1-1/4/5/7/11 were silenced simultaneously because of the sequence similarity between them (Figure S7a,b). When inoculated with *P. capsici*, the lesions were significantly larger in *N. benthamiana* leaves expressing RNAi::RABE1-7 than the RNAi::GUS control (Figure 4a), indicating the positive role of RABE1-1/4/5/7/11 in plant resistance to *P. capsici* infection. To further investigate the function of RABE1-7, we generated a synthetic version of RABE1-7 (RABE1-7<sup>syn</sup>) with shuffled synonymous codon sequences for RNAi evasion (Figure S7c). In leaves expressing the GFP-RABE1-7<sup>syn</sup> construct, GFP-RABE1-7 protein accumulation was not reduced by RNAi::RABE1-7 compared to the RNAi::GUS control (Figure 4b). In contrast, the GFP-RABE1-7 protein was hardly detected in leaves expressing the original RABE1-7 construct and RNAi::RABE1-7 (Figure 4b). These results confirm that the shuffled codons enabled RNAi evasion. *P. capsici* inoculation assays showed that RABE1-7<sup>syn</sup> but not RABE1-7 restored the normal lesion phenotype disrupted by RNAi::RABE1-7 (Figure 4a). These findings further support the conclusion that RABE1-7 is a positive regulator of plant immunity.

## 2.5 | RXLR242 perturbs the secretory pathway of PR1

RABE regulates the secretion of PR1 in *Arabidopsis* (Speth et al., 2009). To assess whether RABE1-7 also influences PR1 secretion, the signal peptide of PR1 was fused in-frame with the N-terminus of red fluorescent protein (PR1-RFP) and expressed in *N. benthamiana* leaves expressing RNAi::RABE1-7 or the RNAi::GUS control. The subcellular localization of PR1-RFP was examined using confocal microscopy. We detected PR1-RFP in the periphery of RNAi::GUS-expressing cells, whereas PR1-RFP fluorescence was consistent with that of the ER marker GFP-HDEL when RABE1-7 was silenced, indicating its mislocalization to the ER membrane (Figure 5a). The subcellular localization of PR1-RFP RABE1-7<sup>syn</sup> was restored to normal (Figure 5a). These results confirm that RABE1-7 is essential for PR1 secretion.

We considered that RXLR242 might disrupt the host protein secretory pathway to interact with RABE1-7. We therefore examined whether RXLR242 interferes with PR1 secretion. Co-expressed GFP-RXLR242 and PR1-RFP translocated the red fluorescence signals from the apoplast region to the ER, and RXLR242 dose-dependently promoted PR1-RFP localization to the ER (Figure 5b). Furthermore, the immunoblotted intercellular fluid from the leaves expressing the indicated constructs showed that the apoplastic and cytoplasmic PR1-RFP accumulation correlated negatively and positively with the RXLR242 doses, respectively (Figure 5c). Taken together, these findings indicate that RXLR242 inhibited PR1 secretion to the apoplast, possibly via interaction with RABE1-7. We assessed whether RXLR242 affects the secretion of other proteins, including LyRCR3 (required for *Cladosporium fulvum* resistance 3) and LyP69B (subtilisin-like protease P69B) from tomato, Plant Natriuretic Peptide A (PNPA) from *A. thaliana*, and NbSBT5.2 (subtilase 5.2) from *N. benthamiana*. These proteins

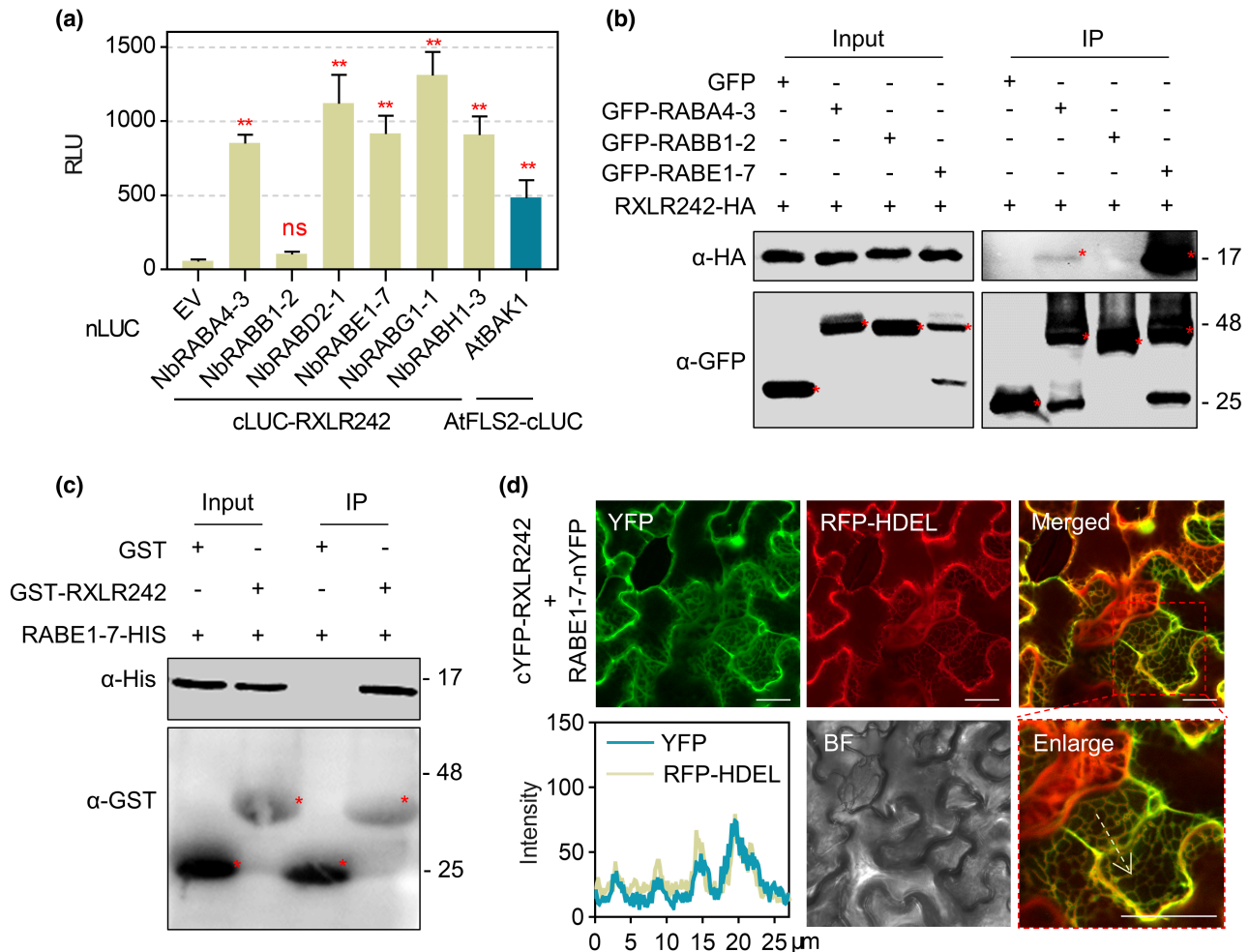


**FIGURE 3** RXLR242 interacts with RAB proteins. (a) Dynamic interactions between RXLR242 with RAB proteins. Luciferase complementation assay was performed on *Nicotiana benthamiana* plants by *Agrobacterium*-mediated transient expression of the indicated constructs. The relative luminescence units (RLUs) of each combination were calculated by a microplate reader (mean  $\pm$  SD,  $n = 3$ ). (b) Verification of the interactions between RXLR242 and three RAB proteins by co-immunoprecipitation (Co-IP) assays. Total proteins were extracted from *N. benthamiana* leaves expressing the indicated proteins. Interacting protein complexes were immunoprecipitated with  $\alpha$ -GFP (green fluorescent protein) beads and the bound proteins were detected by immunoblotting. (c) Verification of the interaction between RXLR242 and RABE1-7 by a pull-down assay. The recombinant glutathione S-transferase (GST) or GST-RXLR242 proteins were expressed in bacteria and purified with  $\alpha$ -GST beads. The RABE1-7-HIS protein was then incubated with the GST precipitate. The pull-down of RABE1-7-HIS was detected using an anti-His antibody by immunoblotting. (d) Verification of the interaction between RXLR242 and RAB proteins by bimolecular fluorescence complementation (BiFC) assays. Indicated constructs were expressed in *N. benthamiana* leaves through agroinfiltration. Confocal microscopy images of indicated leaves were taken at 48 h postinfiltration using a 20 $\times$  lens. Each confocal microscopy picture represents a stack of five single slices. Scale bar = 25  $\mu$ m. The fluorescence plots show relative fluorescence along the dotted lines in the image.

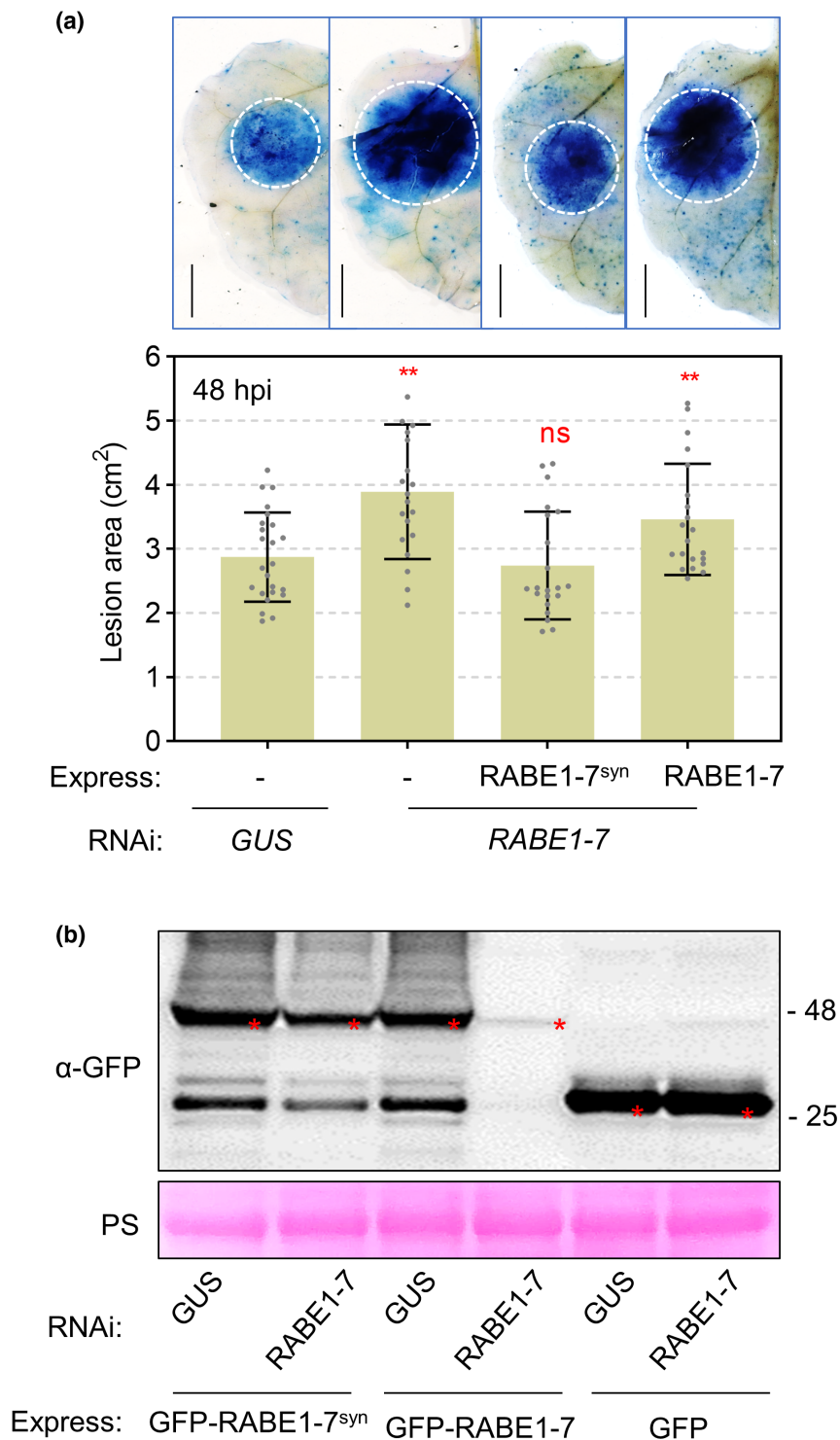
are secreted resistance-conferring proteins involved in interactions between plants and bacteria or oomycete pathogens (Lee et al., 2020; Paulus et al., 2020). We found that RXLR242 inhibited the secretion of LyRCR3 and PNPA but not that of NbSBT5.2 and LyP69B (Figure S8).

To analyse whether *P. capsici* blocked the secretion pathway during infection, we inoculated *P. capsici* mycelium in leaves expressing PR1-RFP (Figure S9). Western blot analysis revealed reduced amounts of apoplastic PR1-RFP in the presence of *P. capsici*, indicating that it blocked the secretion pathway during infection.

## 2.6 | RXLR242 has no effect on the protein stability and GTPase activity of RABE1-7

We explored the mechanism of RXLR242-mediated inhibition of RABE1-7 function. Because multiple RXLR effectors manipulate host immunity by disrupting the turnover of their target proteins (Jing et al., 2016; Park et al., 2012), we initially investigated the effects of RXLR242 on RABE1-7 stability. Immunoblots of *N. benthamiana* leaves co-expressing GFP-RABE1-7 with RXLR242-HA or the empty vector (EV) did not reveal any visible effects of

**FIGURE 4** RABE1-7 positively regulates plant immunity. (a) Enhanced *Phytophthora capsici* infection in RABE1-7-silenced plants. The leaves expressing indicated constructs for 24 h were inoculated with *P. capsici* and were collected at 48 h postinoculation (hpi) for trypan blue staining. The photographs were taken at bright field. Lesion areas at 48 hpi were calculated from three biological replicates using at least four leaves in each replicate (mean  $\pm$  SD,  $n > 12$ ,  $**p < 0.01$ , Student's *t* test). (b) Immunoblot analysis. The total proteins were extracted from leaves expressing indicated constructs. The  $\alpha$ -GFP antibody was used to detect the expression of indicated proteins. Equal loading of each sample is indicated by Ponceau S staining (PS) of the RuBisCO protein.



RXLR242 on RABE1-7 accumulation (Figure 6a). Given that the GTPase activity of RAB proteins is required for their normal function (Nielsen, 2020), we examined whether RXLR242 inhibits the GTPase activity of RABE1-7. We found that RABE1-7-HIS had more GTPase activity than the buffer or GST controls (Figure 6b), which validated its annotation. Adding graded doses of GST-RXLR242 did not affect the GTPase activity of RABE1-7-HIS (Figure 6b), indicating that RXLR242 affects RABE1-7 function via an alternative pathway.

## 2.7 | RXLR242 prevents RABE1-7 from interacting with vesicle-related proteins

Because RAB GTPases function by converting GTP- and GDP-bound states (Nielsen, 2020), we investigated which conformation of RABE1-7 RXLR242 interacted with. We generated RAB mutants that mimic the active (RABE1-7<sup>Q74L</sup>) GTP-bound and inactive (RABE1-7<sup>S29N</sup>) GDP-bound conformations, and examined their associations with RXLR242. The Co-IP results showed that RXLR242 interacted

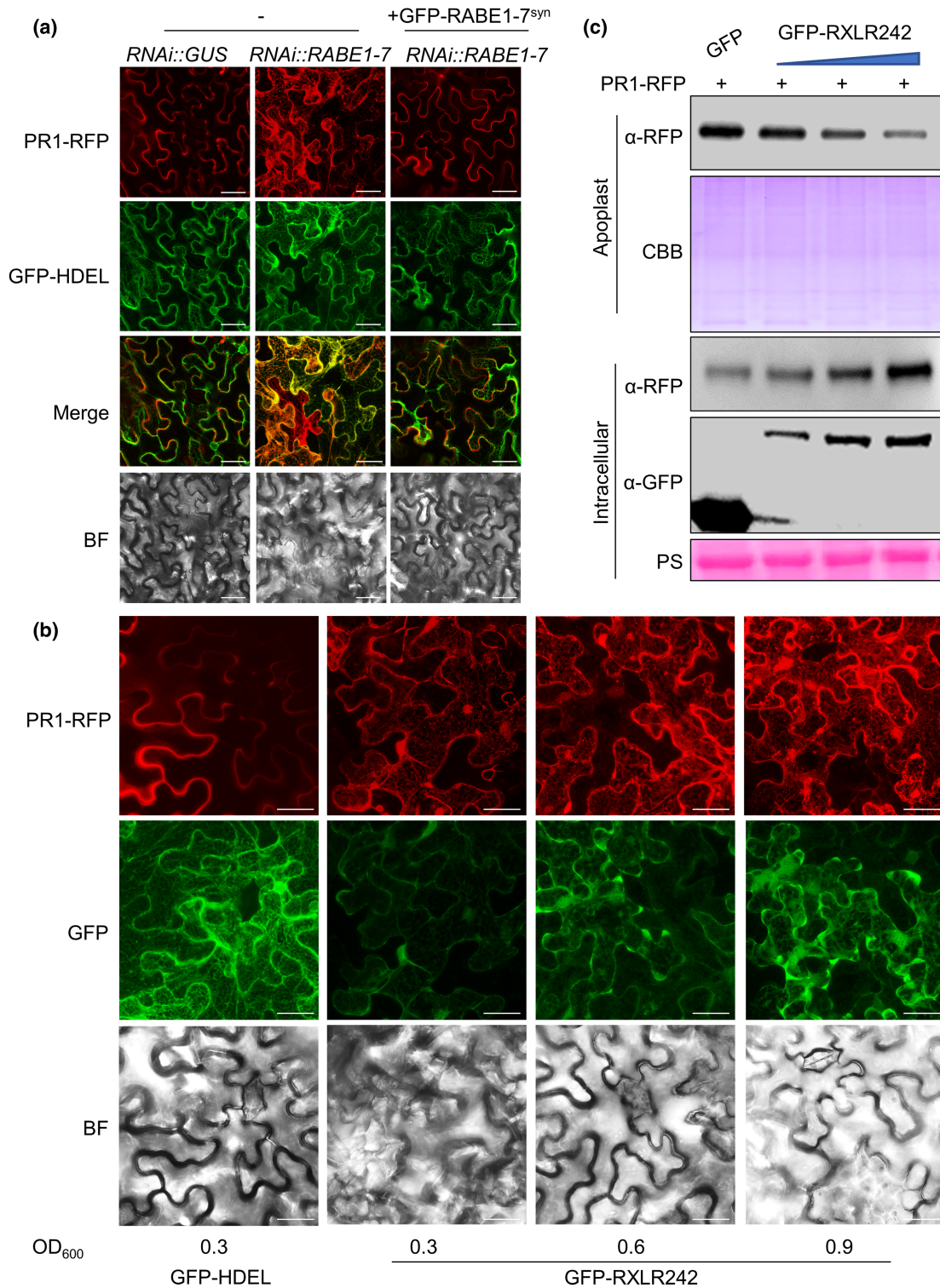


**FIGURE 5** RXLR242 inhibits the RABE1-7-dependent secretion pathway. (a) Secretion of PR1-RFP (red fluorescent protein) depends on RABE1-7. PR1-RFP and the endoplasmic reticulum marker GFP-HDEL were co-expressed in plants harbouring *RNAi::GUS*, *RNAi::RABE1-7* or *RNAi::RABE1-7/GFP-RABE1-7<sup>syn</sup>*. Confocal microscopy images were taken at 48 h postinfiltration (hpi) using a 20× lens. Scale bar = 25 μm. Each picture represents a stack of five single slices. (b, c) RXLR242 inhibits PR1 secretion in a dose-dependent manner. The impact of RXLR242 on PR1-RFP localization was analysed in agroinfiltrated *Nicotiana benthamiana* leaves. The OD<sub>600</sub> values for agroinfiltration were 0.3 for PR1-RFP, 0.3/0.6/0.9 for GFP-RXLR242, and 0.3 for the empty vector (GFP-HDEL). The pictures in (b) were taken at 48 hpi. Scale bar = 25 μm. Each confocal microscopy picture represents a stack of five single slices using a 20× lens. (c) The indicated protein abundance detected by western blot assay. The apoplastic fluid of leaves expressing indicated proteins was collected and the α-RFP antibody was used to detect the PR1-RFP in the apoplast. Equal loading of each sample is indicated by Coomassie brilliant blue (CBB) staining. Intracellular leaf extracts were collected from leaves in which the apoplastic fluid was removed. The α-GFP and α-RFP antibodies were used to detect the expression of indicated proteins. Equal loading of each sample is indicated by Ponceau S staining (PS) of the RuBisCO protein.



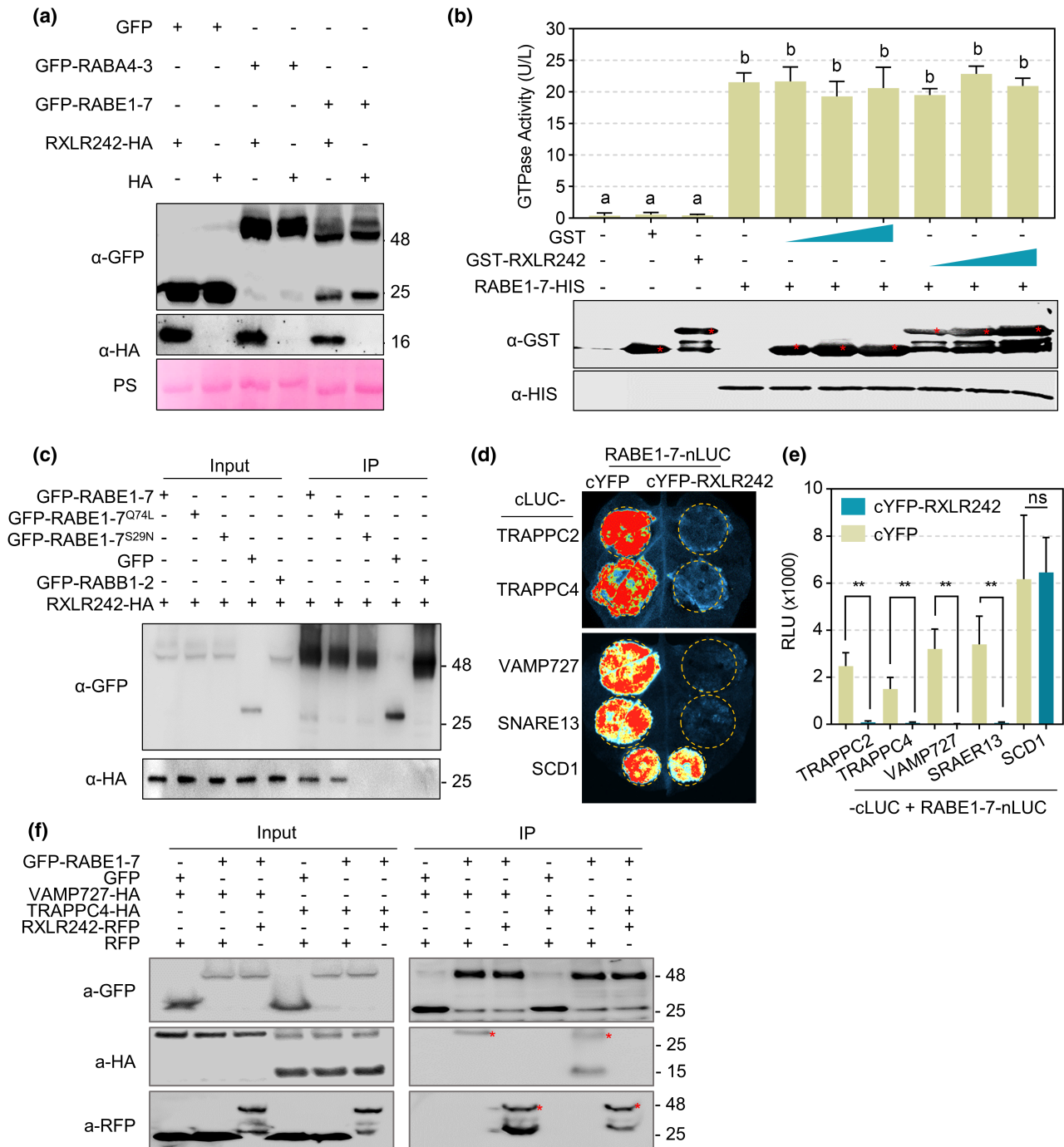


**FIGURE 6** RXLR242 inhibits the interaction of RABE1-7 and vesicle-related proteins. (a) RXLR242 does not affect the protein stability of RABE1-7 or RABA4-3. Total proteins were extracted from *Nicotiana benthamiana* leaves expressing GFP-RABA4-3/GFP-RABE1-7 and RXLR242-HA and detected by western blot. (b) RXLR242 does not affect the GTPase activity of RABE1-7. GST-RXLR242 and RABE1-7-HIS were expressed in *Escherichia coli*. The GTPase activities of RABE1-7 samples are shown on the top panel. Protein loadings are shown on the bottom panel. (c) The interaction between RXLR242 and GTP-bound RABE1-7. RXLR242-HA was transiently co-expressed with GFP-RABE1-7, GFP-RABE1-7<sup>Q74L</sup>, GFP-RABE1-7<sup>S29N</sup> or the GFP control. GFP-RABB1.2 was used as a negative control. Total proteins were extracted at 48 h postinfiltration (hpi). Immunoprecipitations were performed using  $\alpha$ -GFP beads. Tagged proteins were detected by western blot. (d, e) RXLR242 prevents RABE1-7 from interacting with its target proteins. Luciferase complementation assay was performed to evaluate the interaction between RABE1-7 and TRAPPC2, TRAPPC4, VAMP727, SNARE13 or SCD1 in the presence or absence of RXLR242. Pictures were taken 48 hpi (d) and relative luminescence units (RLUs) were detected to measure the luminous intensity (e) (mean  $\pm$  SD,  $n = 8$ ,  $*p < 0.05$ , Student's  $t$  test). (f) RXLR242 competitively interacts with RABE1-7 by co-immunoprecipitation assay. Total proteins were extracted from *N. benthamiana* leaves expressing the indicated proteins. Interacting protein complexes were immunoprecipitated with  $\alpha$ -GFP beads and the bound proteins were detected by immunoblotting.

with RABE1-7<sup>Q74L</sup> but not with RABE1-7<sup>S29N</sup> (Figure 6c), suggesting that RXLR242 specifically binds to the active (GTP-bound) conformation of RABE1-7.

RAB binds GTP to recruit its associated vesicle-related proteins and relocates them to protein trafficking vesicles (Nielsen, 2020). The binding signals were notably stronger for RAB-RXLR242 than the positive control (AtFLS-cLUC+AtBAK1-nLUC) in the LCA (Figure 3a), indicating high-affinity interactions. Thus, we postulated that RXLR242 competitively binds RABE1-7 to prevent its interaction with vesicle-related proteins. We therefore transiently expressed RABE1-7 with cYFP-RXLR242 or cYFP-control in *N. benthamiana* leaves, then analysed the effects using immunoprecipitation (IP) assays. Label-free quantification of the MS data (Cox et al., 2014) revealed that cYFP-RXLR242 significantly reduced the abundance of precipitated GFP-RABE1-7 (Figure S10, and Tables S4 and S5). These findings supported our RXLR242 competitive binding model.

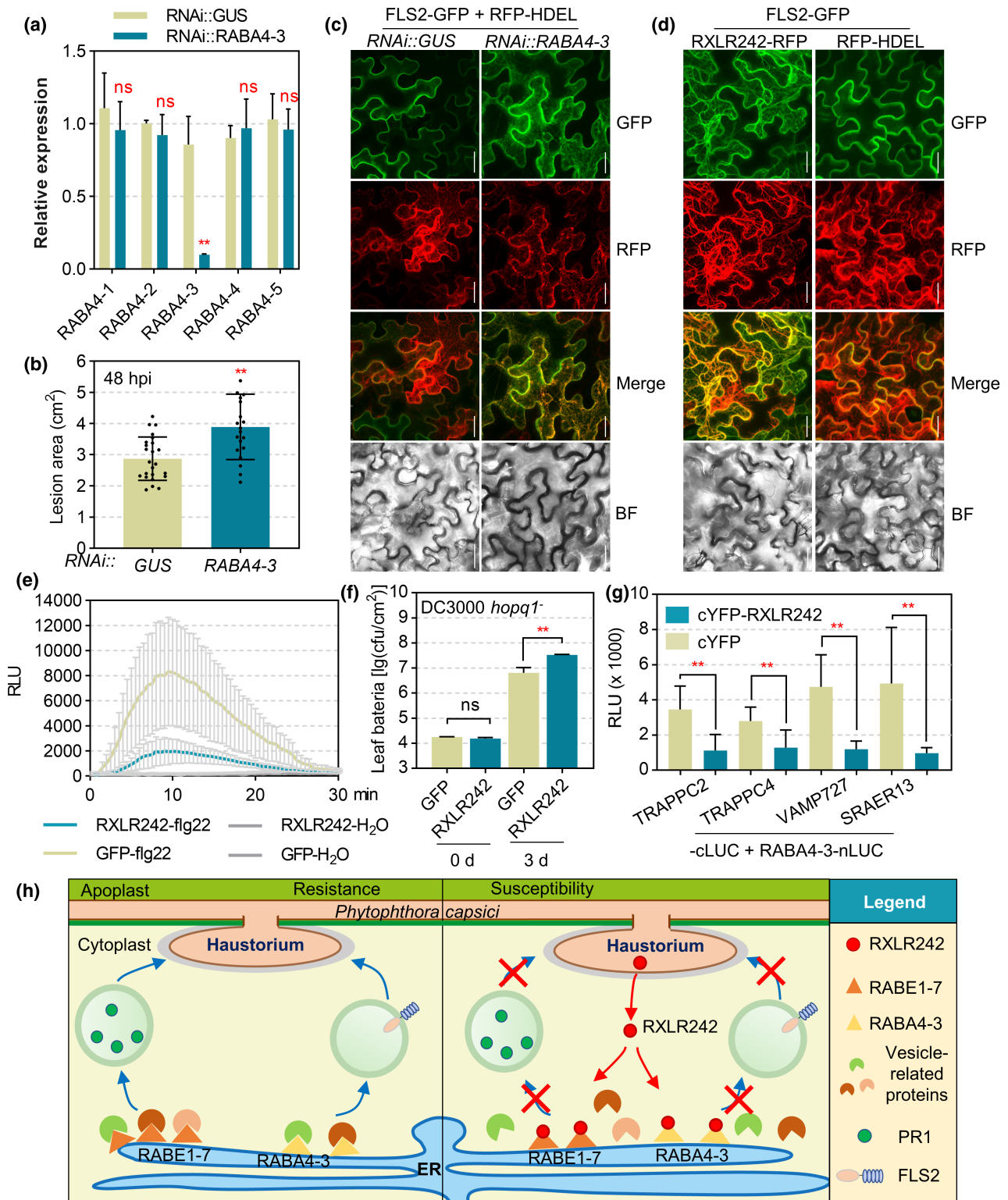
We co-precipitated RABE1-7 with the vesicle-related proteins TRAPPC2, TRAPPC4, VAMP727, and SNARE13 (Table S3), to determine whether RXLR242 disrupts their interactions with RABE1-7. We also examined SCD1, which interacts with RABE in *Arabidopsis* (Mayers et al., 2017), but it was not identified by our IP-MS assay. RXLR242 disrupted the interactions between RABE1-7 and all four targets, but not SCD1 (Figure 6d,e). A Co-IP assay was performed to show further evidence of RXLR242 competitive binding to RABE1-7. VAMP727 and TRAPPC4 were selected for this assay. RABE1-7 co-precipitated with VAMP727 and TRAPPC4 in the absence of RXLR242, indicating that RABE1-7 interacts with VAMP727 and TRAPPC4 (Figure 6f). However, in the presence of RXLR242, little VAMP727 and TRAPPC4 but detectable RXLR242 could be co-precipitated with RABE1-7 (Figure 6f), further supporting that RXLR242 competitively binds to RABE1-7. Collectively, these results indicate that RXLR242 disrupts the host secretion pathway by preventing RABE1-7 from interacting with the vesicle-related proteins and forming trafficking complexes.

## 2.8 | RXLR242 disturbs the trafficking of pattern recognition receptors

In addition to RABE1-7, RABA4-3 is another RXLR242 interactor identified by IP-MS (Table S2) and confirmed by LCA and Co-IP assays (Figure 3a,b). The RABA4 proteins are involved in ER-to-PM trafficking of pattern recognition receptors (PRRs), such as FLS2, in plants (Choi et al., 2013). As a positive regulator of plant resistance (Chaparro-Garcia et al., 2015; Gomez-Gomez & Boller, 2000), FLS2 is a membrane PRR on the cell surface that belongs to a comprehensive network that can monitor potential pathogens (Macho & Zipfel, 2014). FLS2-like protein recognizes the bacterial PAMP flagellin 22 (flg22). The RAB-dependent localization of FLS2 and many other membrane proteins is important for their functions (Gu et al., 2017). Silencing RABA4-3 (Figure 7a) decreased plant resistance to *P. capsici* (Figure 7b) and induced FLS2 retention in the ER without changing FLS2 protein accumulation (Figure 7c, Figure S11), indicating its involvement in FLS2 trafficking.

We then evaluated whether RXLR242 interferes with FLS2 trafficking. Their co-expression partially mislocalized FLS2 from the PM to the ER (Figures 7d and S11), indicating that RXLR242 also disturbs the correct localization of FLS2. Because FLS2 function depends on its PM localization, we postulated that RXLR242-induced FLS2 retention in the ER impairs its recognition of flg22 and host defence response to bacterial infection. This notion was supported by the finding that RXLR242 significantly inhibited the flg22-triggered reactive oxygen species (ROS) burst (Figure 7e). Then we asked whether RXLR242 facilitates colonization of a bacterial pathogen. *N. benthamiana* is a nonhost of *Pseudomonas syringae* DC3000 due to an immune response triggered by the bacterial effector proteins HopQ1, whereas the *P. syringae* DC3000 *hopq1*<sup>-</sup> mutant can infect *N. benthamiana* successfully (Schultink et al., 2017). Leaves expressing GFP-RXLR242 were less resistant to *P. syringae* DC3000 *hopq1*<sup>-</sup> than leaves expressing the GFP control (Figure 7f). Collectively, these results indicate that RXLR242 disrupts the correct localization of PRR.

**FIGURE 7** RXLR242 disturbs the trafficking of pattern recognition receptors. (a) Relative transcript accumulation of RABA4-3 in RABA4-3-silenced leaves. RABA4-3 expression in indicated leaves was analysed by reverse transcription-quantitative PCR with *NbActin* used as a reference (mean  $\pm$  SD,  $n = 3$ , \*\* $p < 0.01$ , Student's  $t$  test). (b) Enhanced *Phytophthora capsici* infection in RABA4-3-silenced plants. Lesion areas at 48 h postinoculation (hpi) were calculated from three biological replicates using at least six leaves in each replicate (mean  $\pm$  SD,  $n > 18$ , \*\* $p < 0.01$ , Student's  $t$  test). (c) FLS2-GFP was co-expressed with RFP-HDEL in leaves harbouring *RNAi::GUS* or *RNAi::RABA4-3*. Each confocal microscopy picture represents a stack of five single slices using a 20 $\times$  lens. Scale bar = 25  $\mu$ m. (d) Mislocalization of FLS2 induced by RXLR242. FLS2-GFP was co-expressed with RXLR242-RFP or RFP-HDEL. Confocal microscopy images show the subcellular localization of FLS2-GFP with (left) or without (right) the presence of RXLR242. Each confocal microscopy picture represents a stack of five single slices using a 20 $\times$  lens. Scale bar = 25  $\mu$ m. (e) RXLR242 inhibits flg22-triggered reactive oxygen species (ROS) burst. GFP-RXLR242 or GFP was transiently expressed in *Nicotiana benthamiana* leaves. Relative luminescence units (RLUs) were measured to track the ROS burst induced by flg22 or water. Each data point consists of eight replicates. Error bars indicate SD. (f) RXLR242 enhances *Pseudomonas syringae* pv. *tomato* DC3000 infection. Colonies of *P. syringae* DC3000 *hopq1*<sup>-</sup> in *N. benthamiana* leaves transiently expressing GFP-RXLR242 or GFP were measured at 0 and 3 days postinoculation (mean  $\pm$  SD,  $n = 8$ , \*\* $p < 0.01$ , Student's  $t$  test). Experiments were carried out three times with similar results obtained. (g) RXLR242 prevents RABA4-3 from interacting with its target proteins. Luciferase complementation assay was performed to evaluate the interaction between RABA4-3 and TRAPPC2, TRAPPC4, VAMP727, SNARE13 in the presence or absence of RXLR242. RLUs were measured (mean  $\pm$  SD,  $n = 8$ , \* $p < 0.05$ , Student's  $t$ -test). (h) A schematic diagram illustrating that RXLR242 disturbs the host protein trafficking pathway by competitively interacting with RABE1-7 and RABA4-3, and finally interfering with the transporting of PR1 and FLS2.



The protein stability of RABA4-3 was unaffected by RXLR242 (Figure 6a). The interaction signals between RABA4-3 and RXLR242 were stronger than those of the positive control in our LCA (Figure 3a), indicating that RXLR242 also suppresses RABA4-3 by competitively binding with it. Given that RABA4-3 and RABE1-7 belong to the same protein family and

are similar (Table S2), we speculated that they share the same vesicle-related interactors. Our LCA results confirmed interactions between RABA4-3 and TRAPPC2, TRAPPC4, VAMP727, and SNARE13 (Figure 7g). Furthermore, RXLR242 also impeded the association between RABA4-3 and these vesicle-related proteins (Figure 7g).

### 3 | DISCUSSION

Filamentous pathogens secrete a diverse array of effectors that target multiple host cell processes to overcome plant immunity and facilitate infection (Dou & Zhou, 2012; Latijnhouwers et al., 2003). Uncovering the mechanisms of how the effectors interfere with the functions of their targets is a critical step towards a comprehensive understanding of host–pathogen interactions. The RXLR effectors characterized by an N-terminal RXLR motif play a major role in the virulence of *Phytophthora* pathogens (Anderson et al., 2015). Here, we characterized and functionally analysed RXLR242, an RXLR effector from *P. capsici*. We found that RXLR242 facilitates *Phytophthora* infection by interacting with RABs, preventing them from binding to their associated vesicle-related proteins and disturbing the trafficking of host defence proteins such as PR1 and FLS2 (Figure 7h).

Compared to the other species, *Phytophthora* pathogens have larger RXLR effector repertoires, most species of which encode hundreds of RXLR effectors (Haas et al., 2009; Jiang et al., 2008). For example, *P. infestans* and *Pythium ultimum* encode 563 and 40 RXLR effectors, respectively (Ai et al., 2020; Haas et al., 2009). However, only a few RXLR effectors are conserved across *Phytophthora* species. Only 16 homologous RXLRs are shared by *P. sojae*, *P. ramorum*, and *P. infestans* (Haas et al., 2009). Moreover, RXLRs are diverse among different strains of the same species. For instance, only 30% of RXLR effectors were found in all the 29 sequenced *P. sojae* genomes (Zhang et al., 2019). In this study, we identified RXLR242 from *P. capsici*, which is highly conserved inter- and intraspecies (Figures S1 and S2). Such effectors are defined as core effectors and might be essential for colonization by *Phytophthora* pathogens (Anderson et al., 2015). Consistent with this, RXLR242 facilitated the *P. capsici* and *P. infestans* infection (Figure 1c,d). The targets of core effectors might function in vital immune pathways that hinder pathogen infection. The interactive targets of RXLR242 regulate the host vesicle-mediated protein trafficking pathways.

*P. capsici* transitions from biotrophy to necrotrophy in *N. benthamiana* at 18–42 hpi (Lamour et al., 2012). The accumulation of RXLR242 transcripts rapidly increased at 6–18 hpi and subsequently declined (Figure 1a). Therefore, RXLR242 probably contributes to the establishment of biotrophy. At this stage, the pathogens need to maintain host-cell vitality and suppress or evade the host defence (Baxter et al., 2010; Mendgen & Hahn, 2002). The tested RXLR242 allele did not induce cell death in *N. benthamiana* and it suppressed the protein trafficking pathway. This RXLR242-mediated breakdown of this pathway probably helps *P. capsici* to establish biotrophy. Notably, RXLR242 did not inhibit all the secreted proteins (Figure S8), indicating that it only disrupts the secretion of specific proteins. Our data also supported the notion that *P. capsici* inhibits the protein secretion pathway during infection (Figure S9).

Plant cells contain various individual membrane-bounded organelles, namely the ER and trans-Golgi network (TGN), the early (EE), late (LE), and multivesicular (MVE) endosomes, and a vacuole. Proteins synthesized de novo are transported from the ER to the

Golgi via vesicles and then to the TGN for delivery to the PM or the apoplast. Intracellular membrane trafficking is essential for plant growth and resistance because of its extensive roles in nutrient uptake, cell wall biosynthesis, and targeting de novo-synthesized enzymes and PR proteins to their correct subcellular destinations (Robatzek, 2007; Tanaka et al., 2006). Vesicular carriers mediate membrane trafficking between the donor and target organelles. This process involves conserved machinery components, including RAB GTPases and a series of vesicle-related proteins (Fujimoto & Ueda, 2012; Hutagalung & Novick, 2011). For example, ARA6/RABF1 plays an important role in trafficking between the PM and MVE in *Arabidopsis*. RAB5/RABF2 mediates endocytic and vacuolar transport pathways (Bottanelli et al., 2011, 2012; Ebine et al., 2011). Furthermore, localized RAB11/RABA proteins in the TGN/EE of *Arabidopsis* and tobacco act on the secretory and endocytic pathways (Berson et al., 2014; Choi et al., 2013). RABA1a participates in the transport of antimicrobial proteins (Tomczynska et al., 2018). RABE1d regulates the secretion of PR1 (Speth et al., 2009). We discovered that RABE1-7 and RABA4-3 participate in trafficking the defence-associated proteins PR1 and membrane-located PRR FLS2, respectively. Silencing RABE1-1/4/5/7/11 or RABA4-3 resulted in PR1 and FLS2 mislocation and accumulation in the ER, respectively (Figures 5a and 7c). Through complementation assays, we successfully proved this function of RABE1-7. Hence, the notion that RABE1-7 and RABA4-3 positively regulate plant resistance to *P. capsici* is well-founded (Figures 4a and 7b). FLS2 is a membrane-located receptor that recognizes a conserved peptide, flg22, from bacteria. However, silencing RABA4-3 still reduced plant resistance to *P. capsici*. There are many other cell surface receptors, such as RLP23, BAK1, and SOBIR1, involved in oomycete pathogen resistance. It is a rational speculation that RXLR242 also inhibits the recycling of these receptors by targeting RABA4-3 and finally promotes infection by *P. capsici*.

RXLR effector interactors are variable and belong to different protein families. RABs are the largest group of small GTPases in plants. The *N. benthamiana* genome encodes 84 proteins that can be grouped into eight subfamilies (RABA-H), and the RABB, RABD, RABE, and RABF subfamilies are expanded in *N. benthamiana* (Figure S5d,e). Notably, the likelihood that most of the putative RXLR242 interactors (62/144) identified by IP-MS are RAB GTPases is low, indicating that RABs are the primary targets of RXLR242. In addition, proteins from all RAB subfamilies (except RABC) interacted with RXLR242, suggesting that RXLR242 broadly targets various RAB types. This broad range of interactions between RXLR242 and RABs was further confirmed by LCA (Figure 3a). More evidence of the association was identified using RABE1-7 and RABA4-3 as representatives (Figure 3b–d). RXLR effectors often target several homologous proteins. For example, Avr3a from *P. infestans* targets the plant cinnamyl alcohol dehydrogenase 7 (CAD7) subfamily (Li et al., 2019). Multiple targets could explain why a single effector can dampen plant immunity.

RABs act as molecular switches by cycling between the active GTP-bound and inactive GDP-bound conformations mediated by

guanine nucleotide exchange factors (GEFs) and GTPase-activating proteins (GAPs), respectively (Barr & Lambright, 2010; Stenmark, 2009; Vernoud et al., 2003). However, RXLR242 did not affect RAB stability or GTPase activity (Figure 6a,b) but might affect the function of RABE1-7 through another pathway by interacting with the GTP-bound conformation of RABE1-7 (Figure 6c).

The GTP-bound forms of RABs can recruit multiple downstream vesicle-associated proteins to form vesicles for intracellular membrane trafficking. Vesicle-associated proteins include sorting adaptors, tethering factors, motor proteins, phosphatases, and kinases that play critical roles in vesicle budding, movement along the actin filaments or microtubules, docking vesicles to the target compartments, and the fusion of acceptor membranes (Eathiraj et al., 2005; Lo et al., 2011). For example, FLS2 trafficking requires RABA4b and its recruited vesicle-related proteins, including phosphatidylinositol 4-kinase (PI4K)  $\beta$ 1, PI4K  $\beta$ 2, and PLANT U-BOX 13 (PUB13) (Antignani et al., 2015). The present study identified putative RAB interactors of RABE1-7 using IP-MS (Figure S10) and found that RXLR242 inhibited the interactions between RABE1-7 and RABA4-3 with their putative effectors (Figures 6e,f and 7g).

In conclusion, the *P. capsici* effector RXLR242 targets RAB GTPases involved in the vesicle-mediated protein trafficking pathway and interacts with RABE1-7 and RABA4-3 to suppress PR1 secretion and trafficking of de novo-synthesized FLS2 to the PM, respectively. We propose a competitive binding model in which *Phytophthora* effectors disturb the RAB-mediated vesicle trafficking by competitively binding RAB GTPases to prevent their interaction with vesicle-related proteins, further inhibiting the trafficking of resistance-related components. Our study provides new insights for future research of RAB protein function in host immunity.

## 4 | EXPERIMENTAL PROCEDURES

### 4.1 | Plant materials and growth conditions

*N. benthamiana* plants were grown and maintained in a greenhouse at 25°C and 60% relative humidity under a 16 h light/8 h dark photoperiod for 5–6 weeks. *Arabidopsis* Columbia-0 (Col-0) plants were grown at 23°C with a 12 h day/12 h night photoperiod for approximately 6 weeks.

### 4.2 | Transient expression in *N. benthamiana*

Recombinant constructs of RXLR242 were transformed into *Agrobacterium tumefaciens* GV3101 and cultured for 36–48 h at 28°C and 220 rpm before infiltration. The cells were collected by centrifugation when the OD<sub>600</sub> was appropriate, washed three times, and then resuspended in 10 mM MgCl<sub>2</sub> to a final OD<sub>600</sub> of 0.2. Five-week-old *N. benthamiana* leaves were infiltrated for transient expression.

### 4.3 | RNAi in *N. benthamiana*

For RNAi, the sense- and antisense-specific segments of indicated genes were cloned into the same p2300 vector at *Kpn* I/*Bam* H I and *Xba* I/*Pst* I restriction sites, respectively. The vector was introduced into *A. tumefaciens* GV3101 by electroporation. *Agrobacterium* suspensions containing the vector were inoculated into the leaves of 30-day-old soil-grown *N. benthamiana*. The silencing efficiency was tested at 48 h postinfiltration.

### 4.4 | Culture and inoculation with *P. capsici*

*P. capsici* LT263 was cultured and maintained at 25°C in the dark on a 10% (vol/vol) V8 juice medium for 3–4 days. Five-millimetre discs containing the growth medium were inoculated with *P. capsici* and placed on agroinfiltrated *N. benthamiana* leaves. The plants were then grown in the greenhouse for 36 h. The inoculated leaves were photographed under UV light, and the lesion areas were measured at 48 h postinoculation (hpi). Each assay was repeated at least in triplicate.

### 4.5 | Protein extraction and western blotting

Agroinfiltrated *N. benthamiana* leaves were harvested at 48 hpi, frozen in liquid nitrogen, ground to a fine powder, and mixed with the extraction buffer (50 mM HEPES, 150 mM KCl, 1 mM EDTA, 0.1% Triton X-100, pH 7.5) supplemented with 1 mM dithiothreitol (DTT) and protease inhibitor cocktail (Sigma-Aldrich). The proteins were fractionated using sodium dodecyl sulphate-polyacrylamide gel electrophoresis (SDS-PAGE) and transferred to 0.2- $\mu$ m polyvinylidene difluoride (PVDF) membranes (Millipore Sigma Co. Ltd) presoaked in methanol for 15 s. Nonspecific protein binding was blocked by shaking the membranes at 40 rpm with Tris-buffered saline (TBS; pH 7.4) containing 3% non-fat dry milk for 1 h at 25°C. Anti-GFP (1:5000 dilution; #M20004) and anti-FLAG (1:5000 dilution; #M20008, both from Abmart Inc.), or anti-RFP (1:1000 dilution; #5f8, ChromoTek) antibodies were added to the blocking buffer and incubated at room temperature for 60–90 min. After three washes with TBS containing 0.1% Tween 20 (TBST) for 5 min each, the membranes were incubated with goat antimouse antibody (1:10,000 dilution; Odyssey no. 926-32210; Li-Cor Biosciences) in TBST at room temperature for 45 min. The membrane was washed three times with TBST and blotted.

### 4.6 | Reverse transcription-quantitative PCR

We evaluated the expression of RABs in RAB-silenced plants. Total RNA was extracted using RNA simple Total RNA Kits (Tiangen) as described by the manufacturer. The cDNA of *N. benthamiana* was synthesized using HiScript II Q RT SuperMix for qPCR (Vazyme Biotech Co. Ltd), then amplified by quantitative PCR using SYBR Premix Ex

Taq Kits (Takara Bio Inc.), three technical replicates, and an ABI Prism 7500 Fast Real-Time PCR system (Thermo Fisher Scientific Inc.) following the manufacturer's instructions. Gene expression levels were normalized to that of *NbACTIN*, a stably expressed reference gene in *N. benthamiana*. The primers used in this study are listed in Table S6.

#### 4.7 | LCA

The coding sequences of the indicated genes were cloned into pCAMBIA1300-35S-HA-Nluc-RBS or pCAMBIA1300-35S-Cluc-RBS (a gift from Prof. Jian-Min Zhou, Chinese Academy of Sciences) and then introduced into *A. tumefaciens* GV3101. We cloned *RXLR242* without the SP region into pCAMBIA1300-35S-Cluc-RBS at *KpnI* and *Sall* restriction sites and *NbRAB*-coding genes into pCAMBIA1300-35S-HA-Nluc-RBS at *SacI* and *Sall* restriction sites. *Agrobacterium* strains harbouring the indicated constructs were infiltrated into *N. benthamiana* leaves. To detect luminescence in leaves, 1 mM luciferin was infiltrated into leaves and the leaves were incubated for 15 min in the dark. The luminescence of whole leaves was detected using a live imager. To calculate the luminescence intensity, leaf discs expressing the constructs were incubated 2 days later with 1 mM luciferin in 96-well plates for 10 min. The luminescence intensity was measured using a microplate reader (BioTek).

#### 4.8 | BiFC assays

The full-length coding sequence of *RXLR242* was cloned into pCAMBIA1300-cYFP to generate the cYFP-*RXLR242* plasmid. *NbRABE1-4*, *NbRABE1-7*, and *NbRABB1.2* were cloned into pCAMBIA1300-nYFP to generate the corresponding nYFP-fused constructs and then transformed into *A. tumefaciens* GV3101. Various combinations were mixed in a 1:1 ratio for injection into *N. benthamiana* leaves. We examined YFP signals using an LSM 700 confocal laser scanning microscope (Carl Zeiss AG).

#### 4.9 | Co-immunoprecipitation assays

Plasmid combinations were transiently expressed in *N. benthamiana* as described above and the leaves were harvested 2 days after agroinfiltration. We co-immunoprecipitated the proteins of interest with anti-GFP and anti-HA affinity beads as described in a previous study (Li et al., 2019). The precipitated proteins were separated by SDS-PAGE and detected by immunoblotting with monoclonal anti-GFP and anti-HA antibodies (Abmart).

#### 4.10 | Protein pull-down assays in vitro

We expressed GST, GST-*RXLR242*, and *NbRABE1-7-HIS* in *Escherichia coli* Rosetta D36E and purified the proteins. For GST

pull-down, 2 ml of the total protein extract containing GST or GST-*PcRXLR242* was incubated with 30  $\mu$ l of glutathione agarose beads (GE Healthcare) at 4°C for 4 h with rotation. The mixture was thoroughly washed twice or three times with TBS buffer containing 0.1% Triton-X-100. After removing the supernatant, the beads were added to the total protein extract containing *NbRABE1-7-HIS* and incubated for an additional 4 h at 4°C. The pull-down of *RABE1-7-HIS* was detected using an anti-His antibody (Abmart).

#### 4.11 | GTPase assay

The GTPase activity of *NbRABE1-7* was measured using ATPase/GTPase assay kits (cat. no. KA1610; Abnova) according to the manufacturer's instructions.

#### 4.12 | Collection of plant apoplastic fluid

The apoplastic fluid from *N. benthamiana* was isolated at 2 days postinfiltration after agroinfiltration. To collect apoplastic fluid from *N. benthamiana* infected by *P. capsici*, 36 h after agroinfiltration the leaves were then inoculated with *P. capsici* before harvesting after a further 12 h. The infiltrated leaves were collected in ice-cold TBS and were infiltrated using a vacuum pump at 60 mbar for 3 min with 2-min intervals at atmospheric pressure to remove all gases. Excess water was removed from the tissues and the leaves were placed in 20-ml syringes placed in 50-ml Falcon tubes on ice. The tubes were centrifuged for 10 min at 1000  $\times$ g at 4°C to extract the apoplastic fluid. All the above steps were performed on ice and the apoplastic fluid was used immediately or frozen and stored at -80°C.

#### 4.13 | Confocal microscopy

Leaves were visualized by microscopy 48 h postagroinfiltration. The agroinfiltrated *N. benthamiana* leaf discs were cut and mounted in distilled water and examined using a laser confocal scanning microscope (LSM 700; Carl Zeiss AG) using 20 $\times$  water or 63 $\times$  oil immersion objectives. Red and green fluorescence emissions were generated at 561 and 488 nm excitation wavelengths, respectively.

#### 4.14 | Oxidative burst assay

The agroinfiltrated and control *N. benthamiana* leaves were cut into 5-mm discs and incubated overnight in 96-well plates containing 200  $\mu$ l of deionized water. The water was removed, and 200  $\mu$ l of luminescence detection buffer (1 mM flg22, 100 mM luminol, and 20 mg/ml horseradish peroxidase) was added. Luminescence intensity was determined after 30 min using a microplate reader (BioTek).



## 4.15 | Trypan blue staining

For trypan blue staining, a stock solution was prepared by mixing 0.02 g trypan blue, 10 g phenol, 10 ml glycerol, 10 ml lactic acid, and 10 ml distilled water. Leaves were soaked in the trypan blue solution overnight at room temperature and then were destained in 95% ethanol for 3 days with gentle shaking. Samples were then equilibrated with 70% (vol/vol) glycerol for photography under white light.

### ACKNOWLEDGEMENTS

We thank Dr Xiangxiu Liang at the Chinese Agricultural University and Dr Meixiang Zhang at Nanjing Agricultural University for their useful suggestions and discussion. The work was supported by the National Natural Science Foundation of China (32070139, 31625023, 31721004, and 32072507) and the Fundamental Research Funds for the Central Universities (KYT202001).

### CONFLICT OF INTEREST

The authors declare no competing interests.

### DATA AVAILABILITY STATEMENT

Detailed sequence information can be obtained from the Oxford Research Archive at <https://ora.ox.ac.uk/objects/uuid:f34c90af-9a2a-4279-a6d2-09cbdc323a2> using the accession numbers (Kourelis et al., 2019) of all *N. benthamiana* genes used in this study (Tables S1–S5). The other sequence data from this article can be found in the GenBank data libraries (<https://www.ncbi.nlm.nih.gov/genbank/>) or Arabidopsis Information Resource (<http://www.arabidopsis.org>) under the accession numbers NbSBT5.2: NbD038072.1; LyRCR3: AAM19207; LyP69B: NP\_001233982; PR1: AT2G14610; FLS2: AT5G46330.1; PNPA: AT2G18660.

### ORCID

Tianli Li  <https://orcid.org/0000-0001-5517-6239>

Gan Ai  <https://orcid.org/0000-0002-2094-5461>

Daolong Dou  <https://orcid.org/0000-0001-5226-6642>

### REFERENCES

- Ai, G., Yang, K., Ye, W., Tian, Y., Du, Y., Zhu, H. et al. (2020) Prediction and characterization of RXLR effectors in *Pythium* species. *Molecular Plant-Microbe Interactions*, 33, 1046–1058.
- Anderson, R.G., Deb, D., Fedkenheuer, K. & McDowell, J.M. (2015) Recent progress in RXLR effector research. *Molecular Plant-Microbe Interactions*, 28, 1063–1072.
- Antignani, V., Klocko, A.L., Bak, G., Chandrasekaran, S.D., Dunivin, T. & Nielsen, E. (2015) Recruitment of PLANT U-BOX13 and the PI4K $\beta$ 1/ $\beta$ 2 phosphatidylinositol-4 kinases by the small GTPase RabA4B plays important roles during salicylic acid-mediated plant defense signaling in *Arabidopsis*. *The Plant Cell*, 27, 243–261.
- Barr, F. & Lambright, D.G. (2010) Rab GEFs and GAPs. *Current Opinion in Cell Biology*, 22, 461–470.
- Baxter, L., Tripathy, S., Ishaque, N., Boot, N., Cabral, A., Kemen, E. et al. (2010) Signatures of adaptation to obligate biotrophy in the *Hyaloperonospora arabidopsidis* genome. *Science*, 330, 1549–1551.
- Beck, M., Heard, W., Mbengue, M. & Robatzek, S. (2012) The INs and OUTs of pattern recognition receptors at the cell surface. *Current Opinion in Plant Biology*, 15, 367–374.
- Berson, T., von Wangenheim, D., Takac, T., Samajova, O., Rosero, A., Ovecka, M. et al. (2014) Trans-Golgi network localized small GTPase RabA1d is involved in cell plate formation and oscillatory root hair growth. *BMC Plant Biology*, 14, 252.
- Boevink, P.C., McLellan, H., Gilroy, E.M., Naqvi, S., He, Q., Yang, L. et al. (2016) Oomycetes seek help from the plant: *Phytophthora infestans* effectors target host susceptibility factors. *Molecular Plant*, 9, 636–638.
- Bottanelli, F., Foresti, O., Hanton, S. & Denecke, J. (2011) Vacuolar transport in tobacco leaf epidermis cells involves a single route for soluble cargo and multiple routes for membrane cargo. *The Plant Cell*, 23, 3007–3025.
- Bottanelli, F., Gershlick, D.C. & Denecke, J. (2012) Evidence for sequential action of Rab5 and Rab7 GTPases in prevacuolar organelle partitioning. *Traffic*, 13, 338–354.
- Chaparro-Garcia, A., Schwizer, S., Sklenar, J., Yoshida, K., Petre, B., Bos, J.I. et al. (2015) *Phytophthora infestans* RXLR-WY effector AVR3a associates with dynamin-related protein 2 required for endocytosis of the plant pattern recognition receptor FLS2. *PLoS One*, 10, e0137071.
- Choi, S.W., Tamaki, T., Ebine, K., Uemura, T., Ueda, T. & Nakano, A. (2013) RABA members act in distinct steps of subcellular trafficking of the FLAGELLIN SENSING2 receptor. *The Plant Cell*, 25, 1174–1187.
- Cox, J., Hein, M.Y., Luber, C.A., Paron, I., Nagaraj, N. & Mann, M. (2014) Accurate proteome-wide label-free quantification by delayed normalization and maximal peptide ratio extraction, termed MaxLFQ. *Molecular & Cellular Proteomics*, 13, 2513–2526.
- Doehlemann, G. & Hemetsberger, C. (2013) Apoplastic immunity and its suppression by filamentous plant pathogens. *New Phytologist*, 198, 1001–1016.
- Dou, D. & Zhou, J.M. (2012) Phytopathogen effectors subverting host immunity: different foes, similar battleground. *Cell Host & Microbe*, 12, 484–495.
- Du, Y., Mpina, M.H., Birch, P.R., Bouwmeester, K. & Govers, F. (2015) *Phytophthora infestans* RXLR effector AVR1 interacts with exocyst component Sec5 to manipulate plant immunity. *Plant Physiology*, 169, 1975–1990.
- Eathiraj, S., Pan, X., Ritacco, C. & Lambright, D.G. (2005) Structural basis of family-wide Rab GTPase recognition by rabenosyn-5. *Nature*, 436, 415–419.
- Ebine, K., Fujimoto, M., Okatani, Y., Nishiyama, T., Goh, T., Ito, E. et al. (2011) A membrane trafficking pathway regulated by the plant-specific RAB GTPase ARA6. *Nature Cell Biology*, 13, 853–859.
- Frei dit Frey, N. & Robatzek, S. (2009) Trafficking vesicles: pro or contra pathogens? *Current Opinion in Plant Biology*, 12, 437–443.
- Fujimoto, M. & Ueda, T. (2012) Conserved and plant-unique mechanisms regulating plant post-Golgi traffic. *Frontiers in Plant Science*, 3, 197.
- Gomez-Gomez, L. & Boller, T. (2000) FLS2: an LRR receptor-like kinase involved in the perception of the bacterial elicitor flagellin in *Arabidopsis*. *Molecular Cell*, 5, 1003–1011.
- Gu, Y., Zavaliev, R. & Dong, X. (2017) Membrane trafficking in plant immunity. *Molecular Plant*, 10, 1026–1034.
- Haas, B.J., Kamoun, S., Zody, M.C., Jiang, R.H., Handsaker, R.E., Cano, L.M. et al. (2009) Genome sequence and analysis of the Irish potato famine pathogen *Phytophthora infestans*. *Nature*, 461, 393–398.
- Hausbeck, M.K. & Lamour, K.H. (2004) *Phytophthora capsici* on vegetable crops: research progress and management challenges. *Plant Disease*, 88, 1292–1303.
- Hutagalung, A.H. & Novick, P.J. (2011) Role of Rab GTPases in membrane traffic and cell physiology. *Physiological Reviews*, 91, 119–149.
- Jiang, R.H., Tripathy, S., Govers, F. & Tyler, B.M. (2008) RXLR effector reservoir in two *Phytophthora* species is dominated by a single rapidly evolving superfamily with more than 700 members. *Proceedings*

- of the National Academy of Sciences of the United States of America, 105, 4874–4879.
- Jing, M., Guo, B., Li, H., Yang, B., Wang, H., Kong, G. et al. (2016) A *Phytophthora sojae* effector suppresses endoplasmic reticulum stress-mediated immunity by stabilizing plant binding immunoglobulin proteins. *Nature Communications*, 7, 11685.
- Jones, J.D.G. & Dangl, J.L. (2006) The plant immune system. *Nature*, 444, 323–329.
- Kamoun, S., Furzer, O., Jones, J.D., Judelson, H.S., Ali, G.S., Dalio, R.J. et al. (2015) The top 10 oomycete pathogens in molecular plant pathology. *Molecular Plant Pathology*, 16, 413–434.
- Kourelis, J., Kaschani, F., Grosse-Holz, F.M., Homma, F., Kaiser, M. & van der Hoorn, R.A.L. (2019) A homology-guided, genome-based proteome for improved proteomics in the allopolyploid *Nicotiana benthamiana*. *BMC Genomics*, 20, 722.
- Kwon, C., Bednarek, P. & Schulze-Lefert, P. (2008) Secretory pathways in plant immune responses. *Plant Physiology*, 147, 1575–1583.
- Lamour, K.H., Stam, R., Jupe, J. & Huitema, E. (2012) The oomycete broad-host-range pathogen *Phytophthora capsici*. *Molecular Plant Pathology*, 13, 329–337.
- Latijnhouwers, M., de Wit, P.J. & Govers, F. (2003) Oomycetes and fungi: similar weaponry to attack plants. *Trends in Microbiology*, 11, 462–469.
- Lee, K.P., Liu, K., Kim, E.Y., Medina-Puche, L., Dong, H., Duan, J., et al. (2020) PLANT NATRIURETIC PEPTIDE A and its putative receptor PNP-R2 antagonize salicylic acid-mediated signaling and cell death. *The Plant Cell*, 32, 2237–2250.
- Li, T., Wang, Q., Feng, R., Li, L., Ding, L., Fan, G. et al. (2019) Negative regulators of plant immunity derived from cinnamyl alcohol dehydrogenases are targeted by multiple *Phytophthora* Avr3a-like effectors. *New Phytologist*. in press. <https://doi.org/10.1111/nph.16139>
- Lo, S.Y., Brett, C.L., Plemel, R.L., Vignali, M., Fields, S., Gonen, T. et al. (2011) Intrinsic tethering activity of endosomal Rab proteins. *Nature Structural & Molecular Biology*, 19, 40–47.
- Macho, A.P. & Zipfel, C. (2014) Plant PRRs and the activation of innate immune signaling. *Molecular Cell*, 54, 263–272.
- Mayers, J.R., Hu, T., Wang, C., Cardenas, J.J., Tan, Y., Pan, J. et al. (2017) SCD1 and SCD2 form a complex that functions with the exocyst and RabE1 in exocytosis and cytokinesis. *The Plant Cell*, 29, 2610–2625.
- Mendgen, K. & Hahn, M. (2002) Plant infection and the establishment of fungal biotrophy. *Trends in Plant Science*, 7, 352–356.
- Minamino, N. & Ueda, T. (2019) RAB GTPases and their effectors in plant endosomal transport. *Current Opinion in Plant Biology*, 52, 61–68.
- Mukhtar, M.S., Carvunis, A.R., Dreze, M., Epple, P., Steinbrenner, J., Moore, J. et al. (2011) Independently evolved virulence effectors converge onto hubs in a plant immune system network. *Science*, 333, 596–601.
- Nielsen, E. (2020) The small GTPase superfamily in plants: a conserved regulatory module with novel functions. *Annual Review of Plant Biology*, 68, 247–272.
- Park, C.H., Chen, S., Shirsekar, G., Zhou, B., Khang, C.H., Songkumarn, P. et al. (2012) The *Magnaporthe oryzae* effector AvrPiz-t targets the RING E3 ubiquitin ligase APIP6 to suppress pathogen-associated molecular pattern-triggered immunity in rice. *The Plant Cell*, 24, 4748–4762.
- Paulus, J.K., Kourelis, J., Ramasubramanian, S., Homma, F., Godson, A., Hörger, A.C., et al. (2020) Extracellular proteolytic cascade in tomato activates immune protease Rcr3. *Proceedings of the National Academy of Sciences of the United States of America*, 117, 17409–17417.
- Petre, B., Contreras, M.P., Bozkurt, T.O., Schattat, M.H., Sklenar, J., Schornack, S. et al. (2021) Host-interactor screens of *Phytophthora infestans* RXLR proteins reveal vesicle trafficking as a major effector-targeted process. *The Plant Cell*, 33, 1447–1471.
- Robatzek, S. (2007) Vesicle trafficking in plant immune responses. *Cellular Microbiology*, 9, 1–8.
- Schmidt, S.M., Kuhn, H., Micali, C., Liller, C., Kwaaitaal, M. & Panstruga, R. (2014) Interaction of a *Blumeria graminis* f. sp. *hordei* effector candidate with a barley ARF-GAP suggests that host vesicle trafficking is a fungal pathogenicity target. *Molecular Plant Pathology*, 15, 535–549.
- Schultink, A., Qi, T., Lee, A., Steinbrenner, A.D. & Staskawicz, B. (2017) Roq1 mediates recognition of the *Xanthomonas* and *Pseudomonas* effector proteins XopQ and HopQ1. *The Plant Journal*, 92, 787–795.
- Speth, E.B., Imboden, L., Hauck, P. & He, S.Y. (2009) Subcellular localization and functional analysis of the *Arabidopsis* GTPase RabE. *Plant Physiology*, 149, 1824–1837.
- Stenmark, H. (2009) Rab GTPases as coordinators of vesicle traffic. *Nature Reviews Molecular Cell Biology*, 10, 513–525.
- Tanaka, H., Dhonukshe, P., Brewer, P.B. & Friml, J. (2006) Spatiotemporal asymmetric auxin distribution: a means to coordinate plant development. *Cellular and Molecular Life Sciences*, 63, 2738–2754.
- Tomczynska, I., Stumpe, M. & Mauch, F. (2018) A conserved RxLR effector interacts with host RABA-type GTPases to inhibit vesicle-mediated secretion of antimicrobial proteins. *The Plant Journal*, 95, 187–203.
- Tsuda, K. & Katagiri, F. (2010) Comparing signaling mechanisms engaged in pattern-triggered and effector-triggered immunity. *Current Opinion in Plant Biology*, 13, 459–465.
- Vernoud, V., Horton, A.C., Yang, Z. & Nielsen, E. (2003) Analysis of the small GTPase gene superfamily of *Arabidopsis*. *Plant Physiology*, 131, 1191–1208.
- Wang, Y. & Wang, Y. (2018) *Phytophthora sojae* effectors orchestrate warfare with host immunity. *Current Opinion in Microbiology*, 46, 7–13.
- Win, J., Morgan, W., Bos, J., Krasileva, K.V., Cano, L.M., Chaparro-Garcia, A. et al. (2007) Adaptive evolution has targeted the C-terminal domain of the RXLR effectors of plant pathogenic oomycetes. *The Plant Cell*, 19, 2349–2369.
- Win, J., Contreras, M.P., Petre, B., Bozkurt, T.O., Schattat, M.H., Sklenar, J. et al. (2019) Host-interactor screens of RXLR effectors reveal plant processes manipulated by *Phytophthora*. *Molecular Plant-Microbe Interactions*, 32, 173.
- Yu, J., Ai, G., Shen, D., Chai, C., Jia, Y., Liu, W. et al. (2019) Bioinformatical analysis and prediction of *Nicotiana benthamiana* bHLH transcription factors in *Phytophthora parasitica* resistance. *Genomics*, 111, 473–482.
- Zhang, X., Liu, B., Zou, F., Shen, D., Yin, Z., Wang, R. et al. (2019) Whole genome re-sequencing reveals natural variation and adaptive evolution of *Phytophthora sojae*. *Frontiers in Microbiology*, 10, 2792.

## SUPPORTING INFORMATION

Additional supporting information can be found online in the Supporting Information section at the end of this article.

**How to cite this article:** Li, T., Ai, G., Fu, X., Liu, J., Zhu, H. & Zhai, Y. et al. (2022) A *Phytophthora capsici* RXLR effector manipulates plant immunity by targeting RAB proteins and disturbing the protein trafficking pathway. *Molecular Plant Pathology*, 23, 1721–1736. Available from: <https://doi.org/10.1111/mpp.13251>